Finite Element Simulations for Entropy Generation Measurement in Single Phase Flow of Water Based Nanofluid Filled in Square Cavity under Appliance of Inclined Magnetic field

S. Bilal (smbilal@math.qau.edu.pk)
Air University

Research Article

Keywords: Entropy generation, Finite element method, Magnetic field, Single phase nano fluid, Square cavity

Posted Date: February 16th, 2021

DOI: https://doi.org/10.21203/rs.3.rs-151378/v1

Finite Element Simulations for Entropy Generation Measurement in Single Phase Flow of Water Based Nanofluid Filled in Square Cavity under Appliance of Inclined Magnetic field

[1*]S. Bilal

[1]Department of Mathematics, Air University, Islamabad, 44000, Pakistan

[* 1*]Corresponding Author: S. Bilal, Email: sardarbilal@mail.au.edu.pk

Abstract: Current communication candidly explicates entropy generation process generated due to natural convective heating in square enclosure saturated with nanofluid. Water is used as base fluid and Cu particles are induced to depict enhancement in thermo physical characteristics. Natural convection in enclosure is produced by providing temperature difference on boundaries. Upper wall is provided uniform temperature while rest of walls are kept cold. Impermeability and non-slip conditions are imposed on all walls. Mathematical structuring of considered problem is manifested via continuity, momentum and energy equations under appliance of inclined magnetic field. Thermo physical properties of nanoparticles along with base liquids are used during mathematical structuring. Finite element procedure is adopted to elucidate flow features. Discretization of domain is done by applying hybrid meshing. Velocity and isothermal plots are drawn against concerning parameters. Comprehensive description of energy generation by measuring variation in magnetic, viscous, total and thermal irreversibility's are also presented. Cut lines representing velocity field in horizontal and vertical direction are also drawn to predict flow behavior at different locations.

Keywords: Entropy generation; Finite element method; Magnetic field; Single phase nano fluid; Square cavity

1 Introduction

Entropy is the intrinsic property of every thermo dynamical system which measures randomness generated due to irreversibility process during thermal energy exchange. Measurement about entropy in thermalized systems is consequence of second thermo dynamical law [1] which relates that amount of total entropy persist uniformly for reversible processes while for irreversible procedures it increases with time. Clausius [2] was one of the foremost responsible for the development regarding thermo mechanic theory about irreversible processes and introduced the concept of entropy. Bejan [3] was among the foremost one who initially deliberated entropy generation rate by formulating method of thermodynamical optimization. Aiming at the optimization of architecture and better performance of thermo hydraulic systems entropy generation processes are applied to numerous conventional industrial structures. In addition entropy analysis is an influential way to uplift efficiency of heat devices likewise in, heat engine, heat pump, refrigerators, high temperature semiconductors, electronic chips cooling systems,

micro heating channels. On overviewing the essence of entropy generation for measuring thermo dynamical irreversibility's in numerous designs researchers have shown pervasive interest. For example, Kefayati et al. [4] explicated entropy generation in convective flow of nano liquid in an inclining enclosure by implementing LBM. They found that with inclusion of entropy aspects a dimensionless Bejan number is modelled in mathematical formulation. They also disclosed that Bejan number has inverse relation with entropic variations. Parvin et al. [5] measured entropic irreversibility produced in water saturated in odd shaped enclosure with induction of metallic nanoparticles. They revealed influential role of natural convection on entropy variation by expressing relation between Rayleigh and Bejan numbers. Merji et al. [6] and Mahmoudi et al. [7] computationally analyzed execution of entropy in square enclosure embedded with water with fusion of hybridized nanoparticles. They interpreted impression of nanoparticle volume fraction on accumulative entropy process. Armaghani et al. [8] probed features of entropy generation in baffled L-shaped enclosure saturated by water under provision of buoyantly convective thermal differentiated to flow domain along with inclusion of alumina nanoparticles. Zamily et al. [9] studied thermo physical features of water along with addition of TiO_2 particles along with checking variation in entropy randomness by locating heat sources at boundaries in cavity. Bouchouch et al. [10] examined irreversibility in nanofluid (H_2O/Al_2O_3) flow in symmetric enclosure by providing non-isothermal heating through introduction of sinusoidal input. They concluded that entropy diffuses in system more quickly and significantly with consideration of free convection environment. Ashornejad et al. [11] depicted randomness generated among particles of water capitalized as host fluid with insertion of different nature nano sized particles in permeable square cavity. They found that dispersion of solid particles raises entropy change and enhances heat transfer. Sheremet et al. [12] deliberated heat transfer formed due to entropic change in water based nanofluid inside square enclosure by transferring variable wall temperature. Alsabery et al. [13] irreversibility aspects in hybridized nanofluid flow comprising of water as host liquids and alumina as suspended constituents by inserting solid concentric cylinders. They disclosed that significant change appears in entropy with enhancement in Rayleigh number (Ra) which measures dominancy of natural convection. Siavashi et al. [14] capitalized two phase mixture of water and copper particles to quantify entropic feature in free convective flow inside permeable enclosure furnished with fins. Kashyap et al. [15] studied two-phase (water/Cu) flow of nanofluid along with execution of entropy in permeable square cavity governed by Brickman-Darcy model under the restriction of different boundary conditions. Analysis about thermo physical characteristics due to entropy generated in nano liquid in lid driven cavity was manifested by Gibanov et al. [16]. Mansour et al. [17] inspected entropy in hybridized nanofluid (water-Cu-Al_2O_3) in square permeable enclosure under appliance of magnetization. They revealed that nanoparticle volume fraction causes increment in entropy. Rahimi et al. [18] considered thermal aspects of entropy process in (water–CuO) nanofluid inside enclosure furnished with fins and estimated decreases in generated entropy against fractional volume of nanoparticles. Rashidi et al. [19] conducted detailed comparative analysis for entropy in symmetrical heat exchanger. Some recently significant disquisitions on entropy process have been carried out in [20-26].

Nanofluids are shattered suspensions of nano scaled particles in the form of nanotubes, nanofibers and droplets and inducted to raise thermal conductivity of ordinary liquids. From the arrival of nanomechanics, nanoliquids becomes under observation due to their intrinsic eccentric attributes. These characteristics have made them proficient in medicinal processes, hybridized engines, fuel cells, microelectronics and in most fields of nanotechnologies [27-28]. Initially, in 1995 Choi [29] disclosed reference of nanofluids as suspension in base fluid. An extensive overview about

nanoliquids is available like Eastman et al. [30] experimentally discussed uplift in thermal conductivity of host fluid with particles suspended by Choi in study referred in [29]. Specifically, researchers are working on enclosed thermally conducted systems due to their extensive practical utility. Likewise, Ahmed et al. [31] adumbrated thermal dispersion of nanoparticles in single phase liquid saturated in lid driven cavity by finite volume scheme. Sheikholeslami and his collaborators [32-33] have shown significance of nanotechnology by examining possessions and properties with usage of different approaches. Yadav et al. [34] have investigated the onset of magnetized nanofluid by finding numerical simulations for heat transfer enhancement along with stability of nanofluid particles in linear and non-linear way. Khan et al. [35] considered constructal Y shaped design to report thermal control and uplift in split lid driven cavity by implementing finite element analysis. Few though provoking investigations related to nanoliquids are enclosed in [36-41].

Analysis about heat transfer characteristics in convective flow generated by temperature gradient in enclosed domains has intended considerable attention due to gaining significant physical importance. This is their competence to resolve wide applicable processes in geological reservoirs, thermally insulated systems, filtration processes, nuclear waste storing, solidification of castings, liquefaction gases, biofilm growth and so forth. Poulikatos et al. [42] derived actual source for generation of natural convection in flow domain i.e. gravity aspects and also determined different ranges about Rayleigh number which controls convection process. Beckermann et al. [43] probed naturally convective flow inside rectangular cavity. Chen and Cheng [44] achieved computational analysis on free convection in an inclining arc shaped enclosure. November and Nansteel [45] adumbrated free convective flow by prescribing different temperatures at boundaries of domain. For interest of readers few recent studies of natural convection heat phenomenon in different shape enclosures under multiple physical conditions are collected in [46-53].

In present disquisition the author has restricted attention towards explication of entropy generation process by providing inclined magnetic field induction along with inclusion of natural convection process. In this pagination an extensive variation in different types of irreversibility's will be discussed against different effective parameters which is not revealed yet. So, it is hope that this work will serve as referenced study for upcoming research in this direction.

2 Mathematical modelling

We have assumed square cavity of unit dimensions saturated by water along with induction of copper nanoparticles. Density variations in flow domain is included by incorporation of buoyancy term represented by Boussinesq approximation which incorporates the role of natural convection in flow domain. Constant magnetization of magnitude B_o is employed in orthogonal direction to measure maximum change in nanoparticles flow. Upper wall of enclosure is considered to be uniformly heated whereas rest of walls are in colder situation. All the boundaries are at no-slip condition. Physical configuration is exemplified in figure 1.

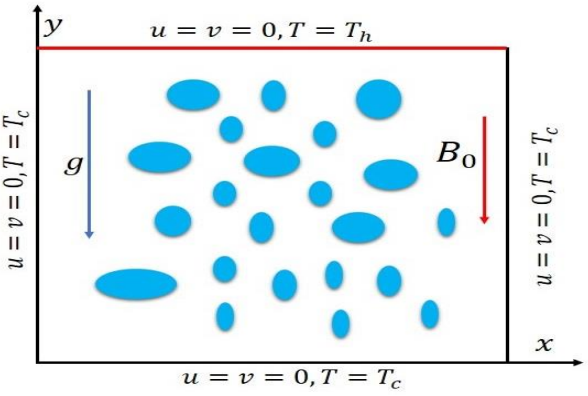

Fig. 1 Physical structuring of problem.

Governing expressions are as follows

$$\frac{\partial u}{\partial x}+\frac{\partial v}{\partial y}=0, \tag{1}$$

$$\frac{\partial u}{\partial \tau}+u\frac{\partial u}{\partial x}+v\frac{\partial u}{\partial y}+\frac{\partial p}{\partial x}= \frac{\mu_{nf}}{\rho_{nf}\alpha_f}\left\{\frac{\partial^2 u}{\partial x^2}+\frac{\partial^2 u}{\partial y^2}\right\}+\frac{\sigma_{nf}}{\sigma_f}\mathrm{Pr}_f\mathrm{Ha}^2\left\{v\sin\gamma\cos\gamma-u\sin^2\gamma\right\}, \tag{2}$$

$$\frac{\partial v}{\partial \tau}+u\frac{\partial v}{\partial x}+v\frac{\partial v}{\partial y}+\frac{\partial p}{\partial y}=\frac{\mu_{nf}}{\rho_{nf}\alpha_f}\left\{\frac{\partial^2 v}{\partial x^2}+\frac{\partial^2 v}{\partial y^2}\right\} +\frac{(\rho\beta)_{nf}}{\rho_{nf}\beta_f}Ra_f\,\mathrm{Pr}_f\,T+\frac{\sigma_{nf}}{\sigma_f}\mathrm{Pr}_f\mathrm{Ha}^2\left\{u\sin\gamma\cos\gamma-v\cos^2\gamma\right\}, \tag{3}$$

$$\frac{\partial T}{\partial \tau}+u\frac{\partial T}{\partial x}+v\frac{\partial T}{\partial y}=\frac{\alpha_{nf}}{\alpha_f}\left\{\frac{\partial^2 T}{\partial x^2}+\frac{\partial^2 T}{\partial y^2}\right\} \tag{4}$$

Thermo physical features concerning to capitalized nanofluid are given respectively

$$\rho_{nf}=(1-\phi)\rho_f+\phi\rho_s, \tag{5}$$

$$(\rho\beta)_{nf}=(1-\phi)(\rho\beta)_f+\phi(\rho\beta)_s, \tag{6}$$

$$(\rho c_p)_{nf}=(1-\phi)(\rho c_p)_f+\phi(\rho c_p)_s, \tag{7}$$

Brickman model for viscosity is utilized represented as follows

$$\frac{\mu_{nf}}{\mu_f} = \frac{1}{(1-\phi)^{2.5}}, \tag{8}$$

Electrical conductivity represented by Maxwell is obliged and expressed as under

$$\frac{\sigma_{nf}}{\sigma_f} = 1 + \frac{3\left[\frac{\sigma_s}{\sigma_f} - 1\right]\phi}{\left[\frac{\sigma_s}{\sigma_f} + 2\right] - \left[\frac{\sigma_s}{\sigma_f} - 1\right]\phi}, \tag{9}$$

Following thermal conductance model is chosen

$$k_{nf} = k_f \left\{1 + \frac{k_s A_s}{k_f A_f} + C k_s Pe \frac{A_s}{k_f A_f}\right\}. \tag{10}$$

Here, Pe and $\frac{A_s}{A_f}$ are the parameters described as follows:

$$Pe = \frac{u_s d_s}{\alpha_f} \text{ and } \frac{A_s}{A_f} = \frac{d_f}{d_s}\left(\frac{\varepsilon}{1-\varepsilon}\right) \tag{11}$$

In Eq. (11), d_f represents the diameter of base and added nanoparticles and shown as follows

$$u_s = \frac{2k_b T}{\pi \mu_f d_s^2}, \tag{12}$$

Associated constraints are as follows

$u = v = p = T = 0,$ in the entire cavity whereas upper wall is at $T_h = 1.$

Entropy production in non-dimensionalized form is given as under

$$S_i = \frac{k_{nf}}{k_f}\left\{\left(\frac{\partial T}{\partial x}\right)^2 + \left(\frac{\partial T}{\partial y}\right)^2\right\} + \psi\left\{2\left(\frac{\partial u}{\partial x}\right)^2 + 2\left(\frac{\partial v}{\partial y}\right)^2 + \left(\frac{\partial u}{\partial y} + \frac{\partial v}{\partial x}\right)^2\right\} + \frac{\sigma_{nf}}{\sigma_f} Ha^2 \psi \left(u \sin\gamma - v\cos\gamma\right)^2. \tag{13}$$

Whereas, Irreversibility ratio ψ is given by:

$$\psi = \frac{\mu_{nf} T_0}{k_f}\left(\frac{\alpha_f}{H\Delta T}\right)^2 \tag{14}$$

In Eq. (14), T_0 is average temperature $T_0 = \frac{T_h + T_c}{2}$.

2. Numerical Procedure

Mathematical modelling containing momentum, heat and entropy expressions are handled with Galerkin finite element scheme. Degree of freedom along with locations for finite element pair is revealed in Fig. 2. As an outcome discrete algebraic intricate algebraic system is attained solved by Newton's method possessing convergence criteria is defined as under

$$\left| \frac{\chi^{n+1} - \chi^{n}}{\chi^{n+1}} \right| < 10^{-6}$$

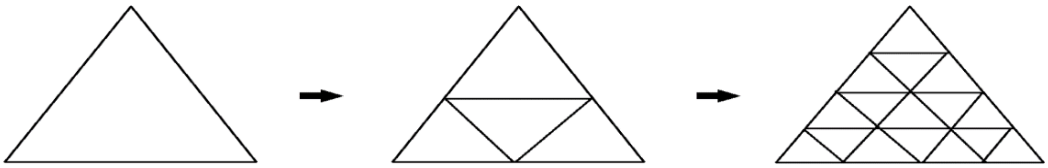

Fig. 2: Sequence of grids on space mesh level: 1, 2, 3 (from left to right)

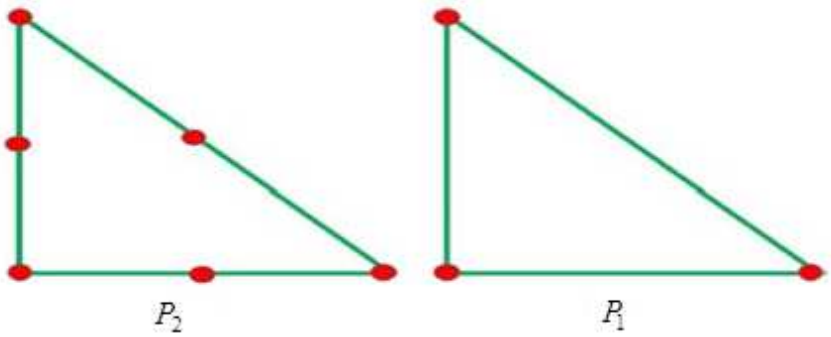

Fig. 3: $P_2 - P_1$ finite element pair with placement of degrees of freedom.

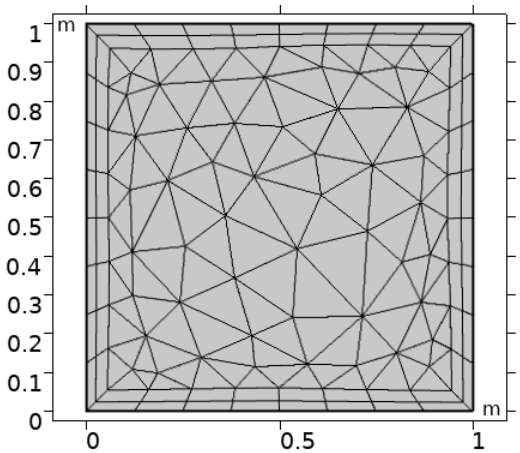

Fig. 4: Discretization of computational domain

Meshing of domain at coarser level of refinement is executed via $P_2 - P_1$ finite element pair for pressure and velocity respectively shown in fig. 3. In addition, complete computational domain is expressed in the form of rectangular and triangular element at coarser level is shown in fig. 4. For computations non-linear system is iterated until the fulfilment of convergence criterion and residual drops by 10^{-6}. Steps carried during implementation of scheme is disclosed in figure 5.

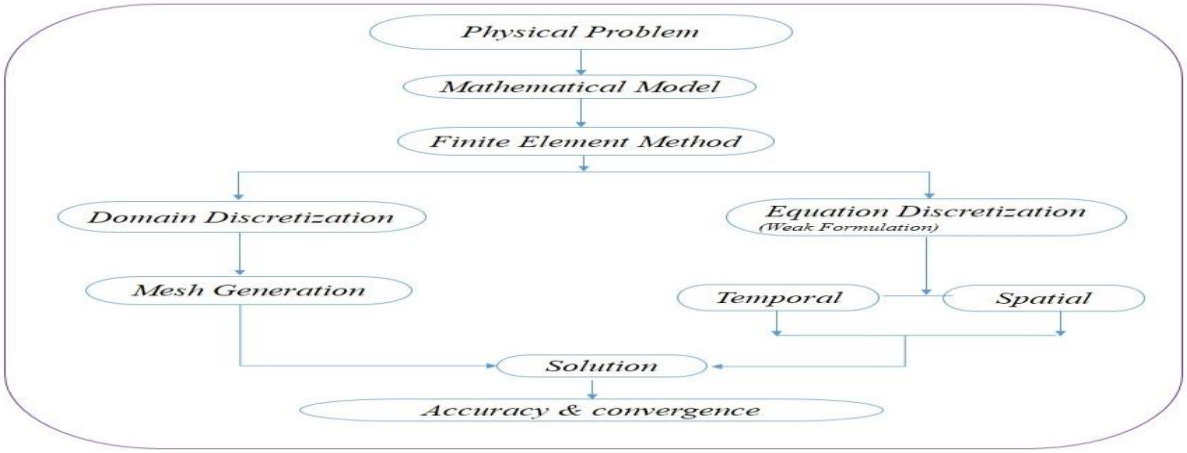

Fig. 5. Step involved in implemented method.

3. Results and Discussion:

This segment is presented to disclose variation in entropy coefficients against flow controlling variables. To gain highly accurate results Galerkin finite element method along with hybridized meshing is executed. Discretization of domain is manifested in the form of triangular and rectangular elements. Data about number of elements along with degrees of freedom are manipulated in table 1 at eight different levels.

Refinement level	Elements	D.O.F
L_1	122	1768
L_2	398	3072
L_3	604	4531
L_4	1094	8036
L_5	1610	11630
L_6	2646	18644
L_7	6268	47831
L_8	30252	180920

Table 1: Variation in Degree of freedom.

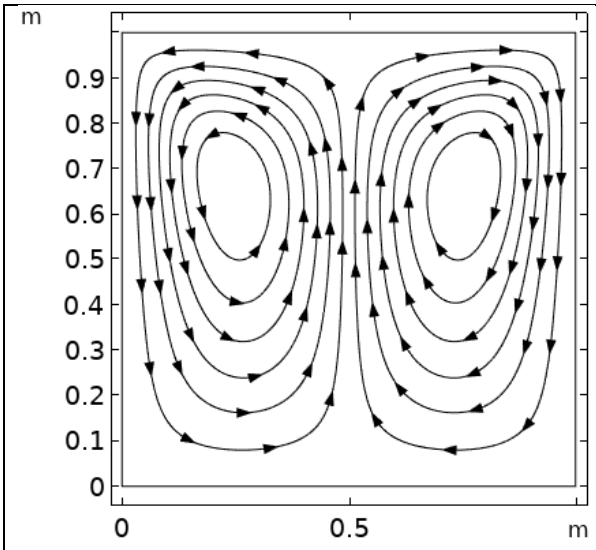

Fig. 6(a)

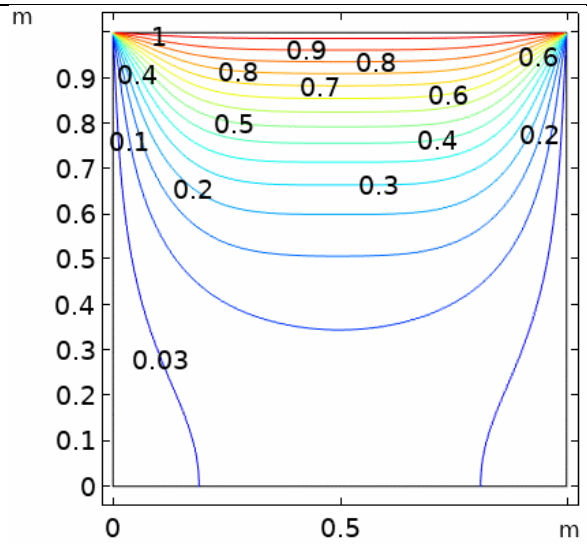

Fig. 6(b)

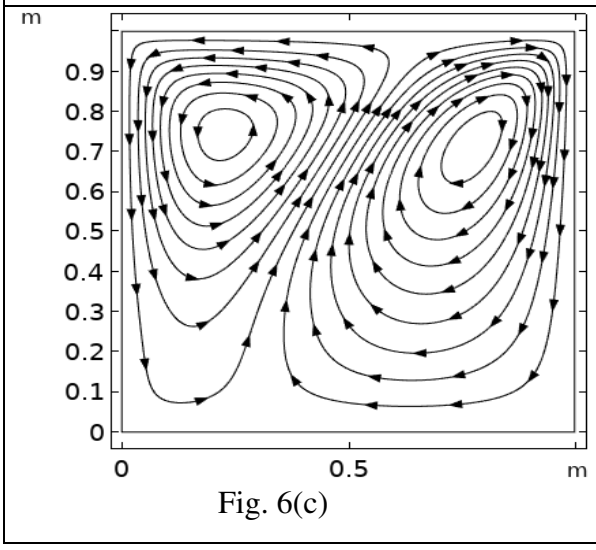

Fig. 6(c)

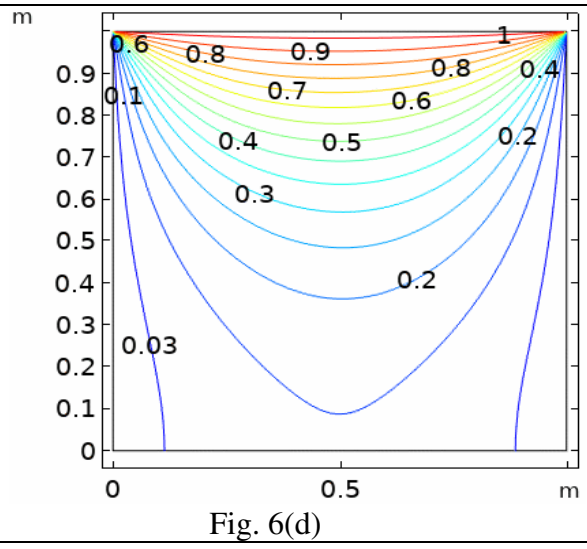

Fig. 6(d)

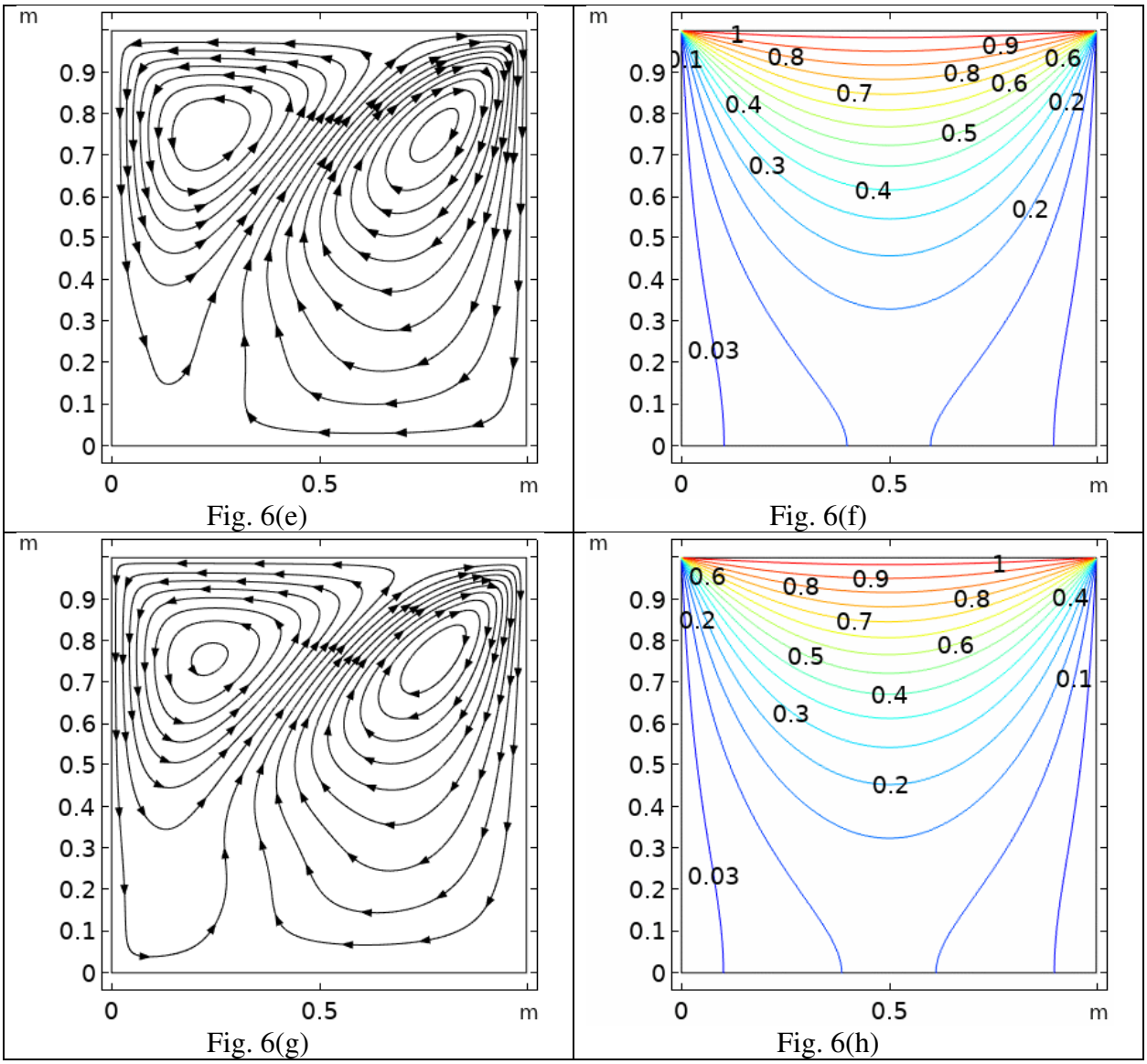

Fig. 6(e) Fig. 6(f)

Fig. 6(g) Fig. 6(h)

Fig. 6(a-h) Influence of Hartmann number (Ha) on streamline (Left) and isotherm (Right)

Figure 6(a-h) shows deviations in stream lines and isotherms pattern for various magnitude of Hartmann number (Ha) varying from $0 \leq Ha \leq 100$ and by fixing nano particles volume fraction $\phi = 0.02$, Rayleigh number Ra=1000, Prandtl number Pr=7. We have noticed the change in concerning line patterns by applying magnetic field at the angle of inclination $\gamma = 30^0$. It is depicted from drawn portray that circular arrangement in flow field is attained that are symmetrical w.r.t mid plane x=0.5 the cell at left side spins in counter clockwise direction, while the cell at right in clockwise direction. It is manifested that with augmentation in Hartmann number the center of coupled cells moves towards top cavity with decline in intensification of lines along with magnitudes. Definitely, the appliance of magnetic field generates a resistive force which translate the entire flow towards vertical axes and reduces the magnitude of flow. Since, in current situation the magnetic field is applied in vertical direction so it has no effect on fluid moving in x direction. Figure 6(a-h) also interprets the change in isotherms by varying magnitude of Hartmann number (Ha). Less relaxation in isotherms is found at lower values of $Ha = 0 \; and \; 40$ whereas, compression appears as we upsurge magnitude of Ha. In current situation we have applied uniform heating at upper wall of enclosure and rest of the walls are kept cold so thermal gradients are generated at upper

boundary. Due to this fact heat is transferred from upper portion of enclosure towards lower. In addition, it is also worthwhile to mention that heat propagate in the form of parabolic structure and propagate in the form of parabolic curve is seen with increment in magnetic field strength. The reason behind the uplift in heat transmission versus Hartmann number (Ha) is that by increasing (Ha) resistive force between fluid molecules enhances and motion of particles restrict and form a collusive environment which raises the temperature field.

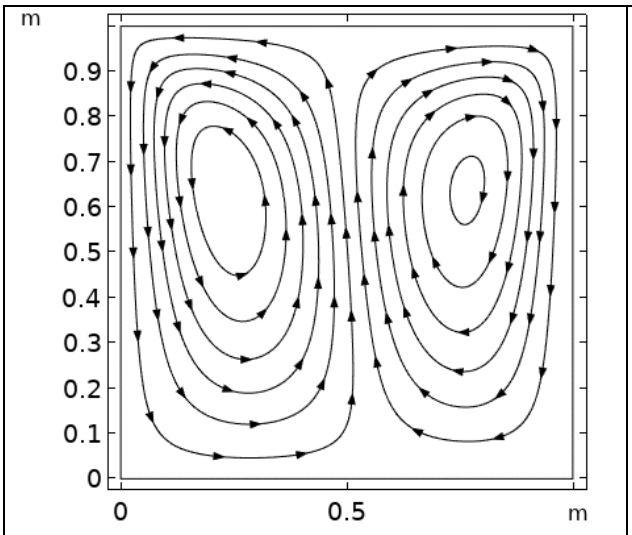

Fig. 7(a)

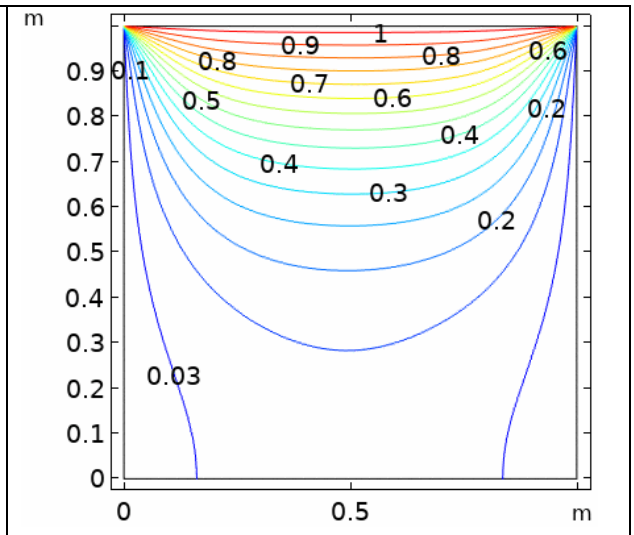

Fig. 7(b)

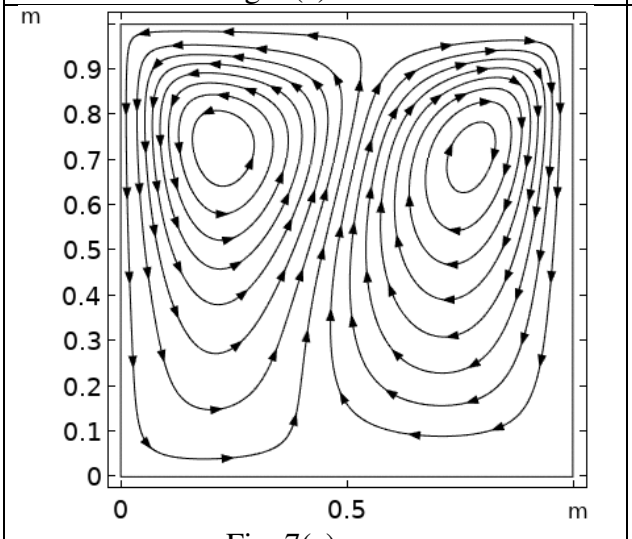

Fig. 7(c)

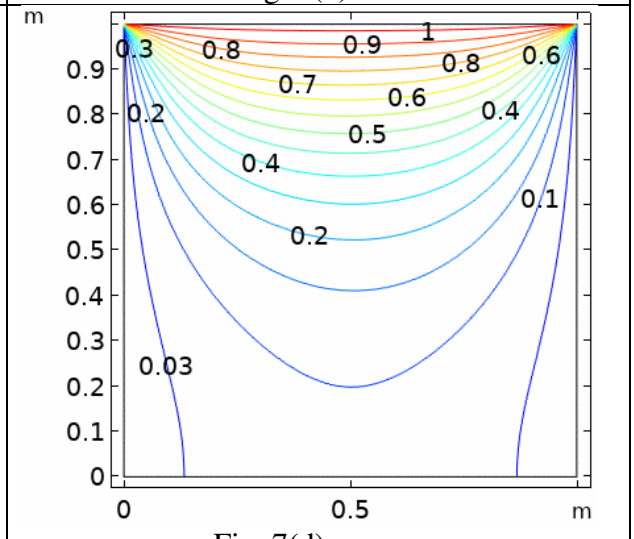

Fig. 7(d)

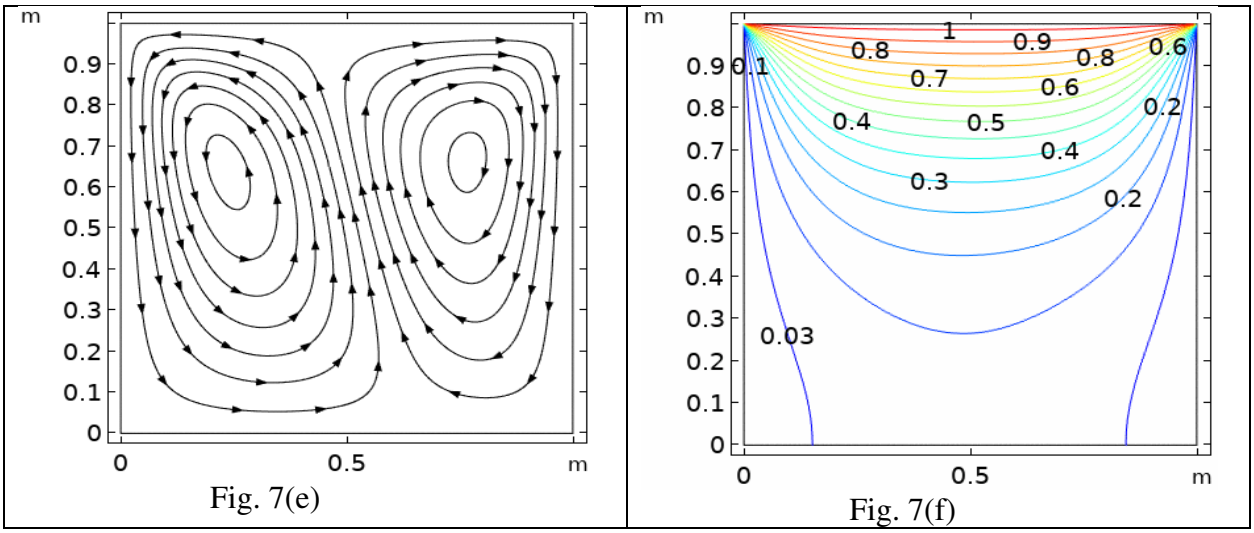

Fig. 7(e) Fig. 7(f)

Fig. 7(a-f) Influence of magnetic field (γ) inclination for streamline (Left) and isotherm (Right).

Figure 7(a-f) elucidates impression of magnetic field inclination angle (γ) varying between $30^0, 60^0, 90^0$ on velocity and temperature fields by drawing circular patterns and isotherms lines respectively. Here, variables like nano particle volume fraction parameter $\phi = 0.02$, Hartmann number $Ha = 20$, Rayleigh number $Ra = 10^6$, Prandtl number $Pr = 7$. It is manifested that by increasing (γ) intensity of fluid circulation represented by streamlines increases because at maximum magnitude of $\gamma = 90^0$ extreme resistance is provided to fluid flow. Symmetrical cells are attained at mid plane $x = 0.5$ at $\gamma = 60^0$ *and* 90^0 and with increase in γ shapes of cells deformed at $\gamma = 60^0$ *and* 90^0. Left hand cells shows anticlockwise movement whereas right hand cells shows clockwise movement.

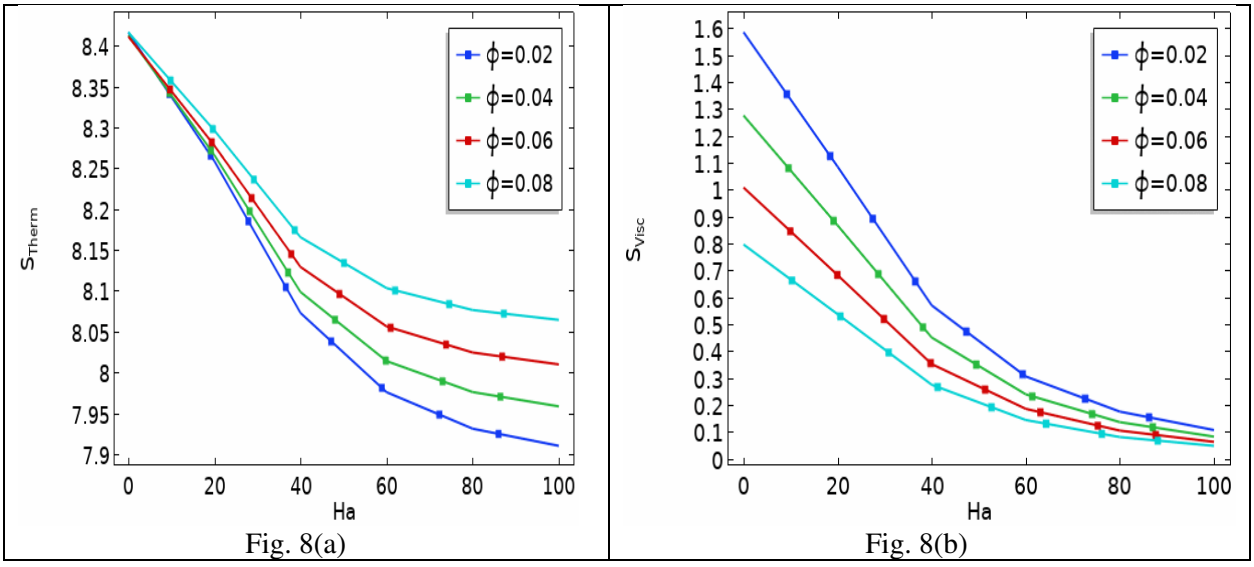

Fig. 8(a) Fig. 8(b)

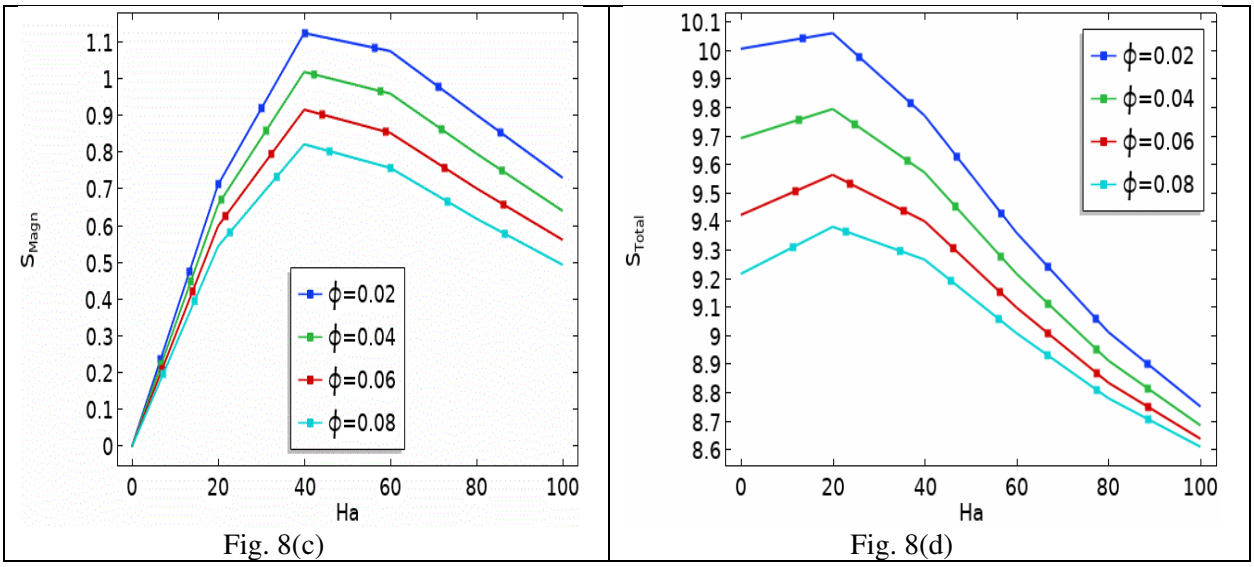

Fig. 8(c) Fig. 8(d)

Fig. 8(a-d) Variation in entropy generation versus ϕ.

In figure 8(a-d) we analyzed the influence of nano particle volume fraction on thermal, viscous, magnetic and total entropy generations along with variation in Hartmann number (Ha). Here, other parameter like $Ra = 1000, \gamma = 30^0, Pr = 7$ are fixed to attain optimized change. In fig. 8(a) we observed that magnitude of thermal entropy generation has constant magnitude for $Ha = 0$ and by increasing values of Ha from $(0.1 \leq Ha \leq 100)$ and by increasing ϕ from $(0.02 \leq \phi \leq 0.08)$ coefficient of entropy change due to temperature gradient decrement. This can be explained by checking deprecating behavior of temperature gradient against increase in ϕ. Behavior of entropy generation due to viscous forces against increasing values of nano particle volume fraction (ϕ) and Hartmann number (Ha) is delineated in fig. 8(b). It is depicted that as we uplift value of (Ha) and (ϕ) decrement (S_{Visc}) curves is manipulated. It is due to the fact as we increase the value of (Ha) viscous forces became dominant and reduction movement of fluid particles enriches as a consequence random generated due to viscous forces decays. It can also be seen that for $Ha > 0$ the magnitude of (S_{Visc}) approaches to zero. Prediction about behavior of entropy generation process to magnetic strength variation in flow field is divulged in fig. 8(c). It is depicted that at $Ha = 0, S_{magn} = 0$ and at certain stage of magnitude of Ha i.e. 40. It reduces to maximum values after attaining maximum amplitude of curves at Ha=40. The magnitude of randomness generated due to magnetic field by influenced by nano particle volume fraction. Impact of nano particle (ϕ) volume fraction and Hartmann number (Ha) depreciates. Impact of nano particle volume fraction (ϕ) and Hartmann number (Ha) on accumulative entropy generation coefficient S_{Total} is discussed in fig. 8(d). It is observed that by increasing (ϕ) and (Ha) in range of $(0.02 \leq \phi \leq 0.08)$ and $(0 \leq Ha \leq 100)$ total entropy coefficient depresses.

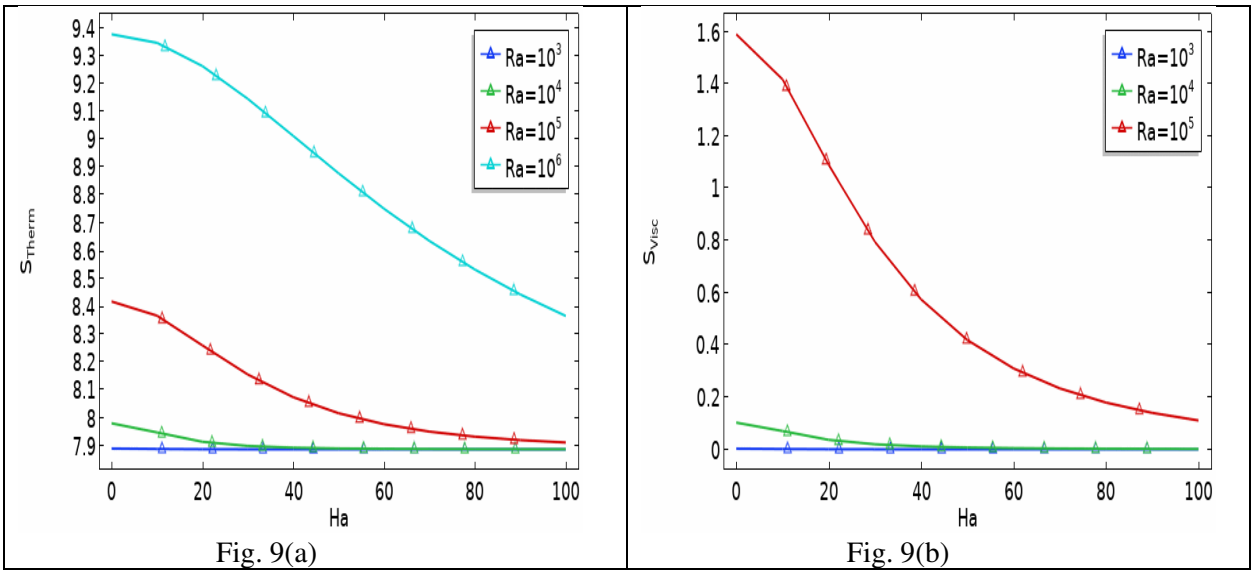

Fig. 9(a) Fig. 9(b)

Fig. 9(a-b) Variation in entropy generation versus (Ra).

Variation in thermal, viscous and magnetic entropy generation against Rayleigh number (Ra) and Hartmann number (Ha) is measured in figure 9(a-b). Hartmann number (Ha) is considered from 0 to 100 and taken along x-axis whereas Rayleigh number is considered from $10^3 to\ 10^6$. Figure 9(a) shows that at constant and maximum magnitude of thermal entropy generation (S_{Therm}) is attained at (Ha = 0) for different magnitudes of Rayleigh number (Ra). It is important to note that when boost to high Hartmann number (Ha) and Rayleigh number (Ra) is provide coefficient of thermal entropy generation reaches asymptotically to zero. The reason behind decrementing behavior of (S_{Therm}) is due to the fact that by increasing Hartmann number (Ha) Lorentz forces are generated which reduces the velocity and temperature gradients in flow field. This reduction in thermal differences reduces thermal irreversibility and at certain stage of (Ha) development of thermal entropy becomes irrelevant. Change in viscous entropy generation coefficient (S_{visc}) versus mounting magnitude of Hartmann number (Ha) and Rayleigh number (Ra) is divulged in fig. 9(b). It is convenient to observe that by fixing nanoparticle volume fraction (φ) the viscous entropy generation decrease against (Ha) whereas uplift is depicted against increasing magnitude of (Ra). This decline in (S_{visc}) is due to decrease in natural convection which is produced due to latent impact of Lorentz force. On other hand, increasing response to (S_{visc}) against (Ra) is due to reason that by increasing (Ra) thermal buoyancy forces are produced which as an outcome generates temperature differences along with randomness of particles in flow domain. In addition it is worthwhile to note that for ($0 \leq Ha \leq 100$) and fixing Ra = 1000 the magnitude of (S_{visc}) remains zero. This shows that by considering low magnitude of (Ra) coefficient of viscous entropy becomes null.

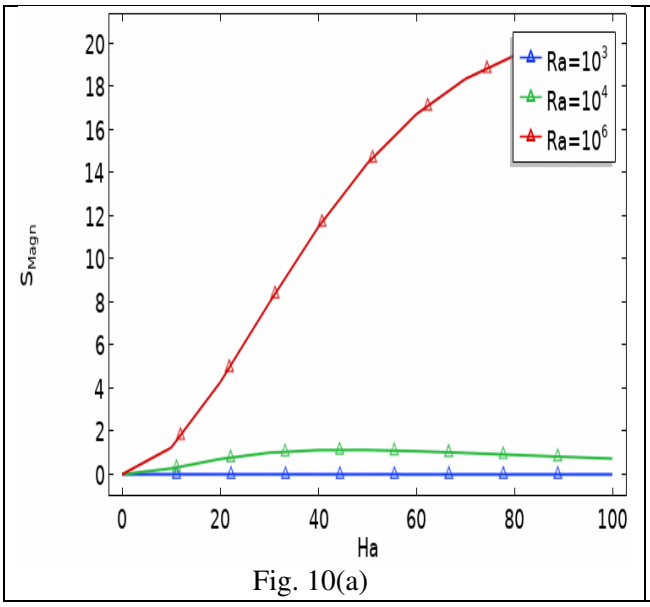

Fig. 10(a)

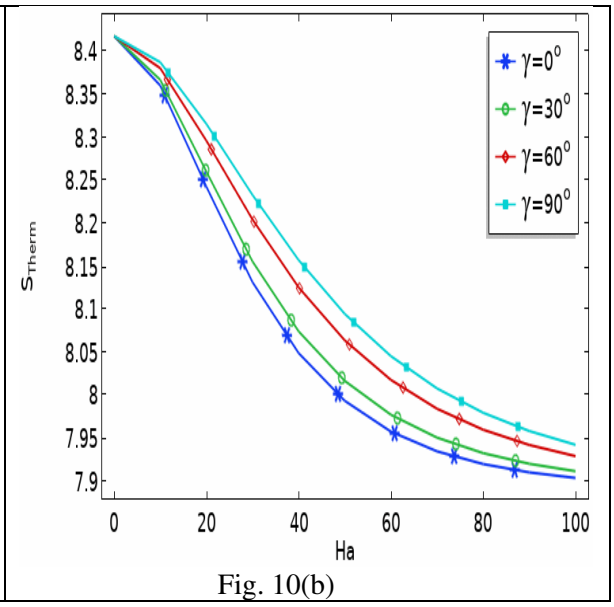

Fig. 10(b)

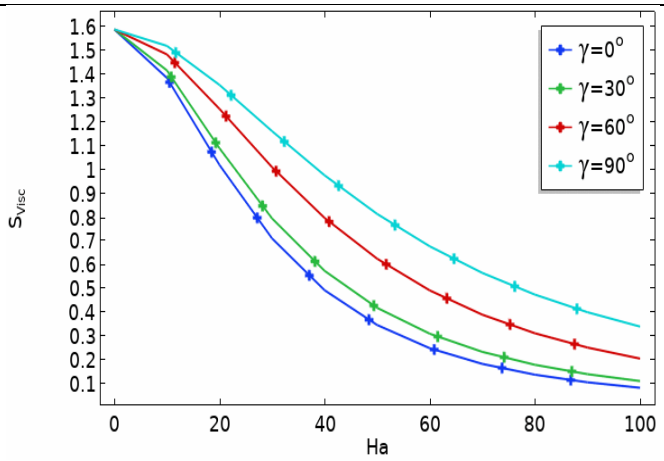

Fig. 10(c)

Fig. 10(a-c) Entropy variation against ($\boldsymbol{\gamma}$)

Fig. 10(a-c) investigates about influence of magnetic field inclination angle ($\boldsymbol{\gamma}$) and Hartmann number (Ha) on thermal, viscous and magnetic irreversibility's is revealed. To see response of irreversibility coefficients in significant way Rayleigh number (Ra) and Prandtl number (Pr) are fixed to 10^6 and 7 respectively. Here, in these sketches $\boldsymbol{\gamma}$=0 represent angles of inclination when magnetic field is applied in direction of x-axis whereas $\boldsymbol{\gamma}=90^0$ shows that it is applied in vertical direction. The considered range for Hartmann number in current figures is between 0 and 100, while inclination angle of magnetic field is ranging from $0^0\ to\ 90^0$. The magnitude of nanoparticle volume fraction is each case is fixed at 4 %. Fig. 10(a) discloses the change in thermal entropy production with respect to Hartmann number (Ha) and magnetic inclination angle ($\boldsymbol{\gamma}$). It is seen from this figure that when (Ha=0) coefficient of thermal entropy reaches to optimum magnitude valued at 8.4 on vertical axis. It is also found that as we increase Hartman number

between 0 and 100 the magnitude of (S_{Therm}) depresses whereas reverse behavior is depicted in case of incrementing magnitude of magnetic field inclination angle ($\boldsymbol{\gamma}$). This can be explained by the augmentation of the thermal gradients via enhancement of convection currents in enclosure with rise in magnetic field inclination angle. Fig. 10(b) represents deviation in curves measuring change in viscous entropy coefficient against magnetic field inclination angle (γ) and Hartmann number (Ha). From view of graph it is explicitly seen that by increasing (Ha), (S_{Visc}) profile down surges but opposite to it uplift is observed in case of magnetic field inclination angle (γ). It is due to the argument that by increasing (γ) temperature difference is enhanced at different portions of enclosure and thermal buoyancy forces are generated which as a conclusion execute convective current. These currents produces enhancement in viscous entropy randomness. With regards to magnetic irreversibility, it has been observed from fig. 10(c) that effect of magnetic field inclination angle on magnetic entropy generation reverses from low Hartmann number ($0 \leq Ha \leq 40$) to high Hartmann number ($40 < Ha \leq 100$). Indeed, this figure discloses a decrease in magnetic entropy measures for weaker Hartmann number and increasing function in case of stronger magnitude of (Ha). It is clear that for constant Hartmann number the effect of inclination angle on magnetic entropy is manifested through Lorentz force proved mathematically from relation provided in eqs. (2.3) and through entropy generation (Eq. 14). Therefore, at low Hartmann number, by increasing inclination angle, magnetic irreversibility dominates by extrinsic character of Lorentz force which is expressed by a decrease in flow velocity. Whereas, at high Hartmann number, the magnetic irreversibility dominates by the key impacts of the effective electric conductivity, which increases by increasing the inclination angles.

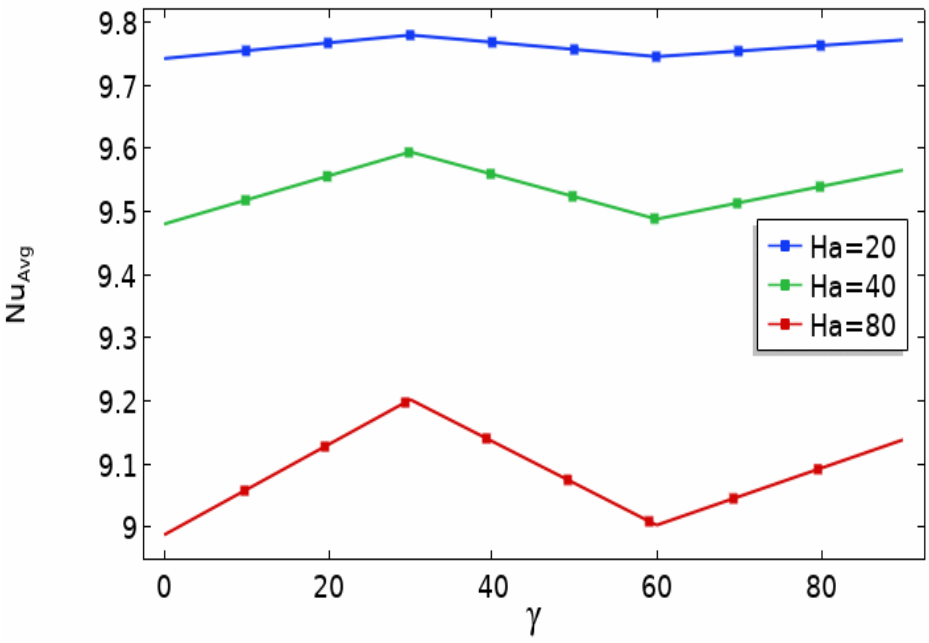

Fig. 11 Influence on average Nusselt number for various Ha.

Variation in heat flux coefficient against increasing magnitude of magnetic field inclination angle ($\boldsymbol{\gamma}$) and Hartmann number (Ha) is divulged in figure 11. Here, it is observed that for different

magnitude of (Ha) and by varying ($\boldsymbol{\gamma}$) between $0^0\ to\ 30^0$ and for $\boldsymbol{\gamma} > 60^0$ average Nusselt number increases.

4. Conclusion:

In current communication we have addressed the phenomenon of entropy production in natural convective heat transfer of Cu-H_2O nanofluid enclosed in square enclosure. Magnetic field is applied at different angles of inclination to measure its impact on irreversibility process. Temperature gradient is provided in flow domain by providing constant heat at upper wall of enclosure while rest of all boundaries are kept cold. Mathematical formulation of under consideration problem is conceded in the form of coupled partial differential system. Solution of governing equations are attained by implementing finite element scheme. Deviation in velocity and temperature fields are discussed by sketching stream and isothermal patterns against involved parameters. Three different types of entropy variations namely; magnetic, viscous and thermal entropies are measured. So, the prime concern of our current effort is to disclose variation in entropy generation in enclosure and prediction about factors effecting entropy measurements.

The key outcomes are itemized below

i) Symmetrical stream line contour at mid plane i.e. x = 0.5 is attained for Ha = 0 and by fixing φ = 0.02 and $\boldsymbol{\gamma}$ = 30^o.
ii) Heat is propagated in the form of parabolic curves and initiated from upper surface of enclosure due to provision of temperature gradient.
iii) Decrementing aptitude of (S_{Therm}) is found against increasing value of nanoparticle volume fraction (φ) for Ha > 0, whereas, for Ha = 0 a constant magnitude of (S_{Therm}) is depicted against each value of (φ) from 0.02 to 0.08.
iv) It is seen that curves representing variations in (S_{Visc}) approaches towards zero with change in (φ).
v) It is adhered that magnetic entropy variation become zero at Ha = 0 while it increases for Ha < 40 and after this critical range it start depreciating.

6. References:

[1] E. Mendoza, “Reflections on the Motive Power of Fire and other Papers on the Second Law of Thermodynamics,” *Dover Publications: New York, NY, USA*, 1988.

[2] R. Clausius, “Mechanical Theory of Heat; Institute of Human Thermodynamics,” *Publishing Ltd. Chicago, IL, USA,* pp. 1850–1865. 2006.

[3] A. Bejan, “Second law analysis in heat transfer,” *Energy*, pp. 720–732, 1980.

[4] G. H. R. Kefayati, N. A. Che Sidik,” Simulation of natural convection and entropy generation of nonNewtonian nanofluid in an inclined cavity using Buongiorno’s mathematical model (Part II, entropy generation),” *Powder Technology*, vol. 305, pp. 679-703, 2017.

[5] S. Parvin, A. J. Chamkha," An analysis on free convection flow, heat transfer and entropy generation in an odd-shapped cavity filled with nanofluid," *International communications in Heat and Mass Transfer*, vol. 54, pp. 8-17, 2014.

[6] I. Mejri, A. Mahmoudi, M. A. Abbasi, A. Omri, "Magnetic field effect on entropy generation in a nanofluidfilled enclosure with sinusoidal heating on both side walls," *Powder Technology*, vol. 266, pp. 340-353m 2014.

[7] A. Mahmoudi, I. Mejri, M. A. Abbasi, A. Omri," Analysis of the entropy generation in nanofluid-filled cavity in the presence of magnetic field and uniform heat generation/absorption," *Journal of Molecular Liquids*, vol. 198, pp. 63-77, 2014.

[8] T. Armaghani, A. Kasaeipoor, N. Alavi, M. M. Rashidi," Numerical investigation of water-alumina nanofluid natural convection heat transfer and entropy generation in a baffled L-shaped cavity," *Journal of Molecular Liquids*, vol. 223, pp. 243-251, 2016.

[9] A. M. J. Al-Zamily, "Analysis of natural convection and entropy generation in a cavity filled with multi-layers of porous medium and nanofluid with a heat generation," *International Journal of Heat and Mass Transfer*, vol. 106, pp. 1218-1231, 2017.

[10] A. E. M. Bouchoucha, R. Bessaïh, H. F. Oztop, K. Al-Salem, F. Bayrak, "Natural convection and entropy generation in a nanofluid filled cavity with thick bottom wall: effect of non-isothermal heating," *International Journal of Mechanical Science*, vol. 126, pp. 95-105, 2017.

[11] H. R. Ashorynejad, B. Hoseinpour, "Investigation of different nanofluids effect on entropy generation on natural convection in porous cavity," *European Journal of Mechanics B/Fluids*, vol. 62, pp. 86-93, 2017.

[12] M. A. Sheremet, T. Grosan, I. Pop, "Natural convection and entropy generation in a square cavity with variable temperature side walls filled with a nanofluid: Buongiorno's mathematical model," *Entropy*, vol. 19, pp. 337, 1-16, 2017.

[13] A. I. Alsabery, M. S. Ishak, A. J. Chamkha, I. Hashim," Entropy Generation analysis and natural convection in a nanofluid-filled square cavity with a concentric solid insert and different temperature distributions," *Entropy*, vol 336, pp. 1-24, 2018.

[14] M. Siavashi, R. Yousofvand, S. Rezanejad, "Nanofluid and porous fins effect on natural convection and entropy generation of flow inside a cavity," *Advanced Powder Technology*, vol. 29, pp. 142-156, 2018.

[16] D. Kashyap, A. K. Dass, "Two-phase lattice Boltzmann simulation of natural convection in a Cu-water nanofluid filled porous cavity: effects of thermal boundary conditions on heat transfer and entropy generation," *Advanced Powder Technology*, vol. 29, pp. 2707-2724, 2018.

[17] N. S. Gibanov, M. A. Sheremet, H. F. Oztop, N. Abu-Hamdeh, "Mixed convection with entropy generation of nanofluid in a lid-driven cavity under the effects of a heat-conducting solid wall and vertical temperature gradient," *European Journal of Mechanics / B Fluids*, vol. 70, pp. 148-159, 2018.

[18] M. A. Mansour, S. Siddiqa, R. S. R. Gorla, A. M. Rashad, "Effect of heat source and sink on entropy generation and MHD natural convection of Al2O3-Cu/water hybrid nanofluid filled with square porous cavity," *Thermal Science and Engineering Progress*, vol. 6, pp. 57-71, 2018.

[19] A. Rahimi, M. Sepehr, M. J. Lariche, A. Kasaeipoor E. H. Malekshah, "Entropy generation analysis and heatline visualization of free convection in nanofluid (KKL model-based) –filled cavity including internal active fins using lattice Boltzmann method," *Computers and Mathematics with Applications*, vol. 75, pp. 1814-1830, 2018.

[20] M. M. Rashidi, M. Nasiri, M. S. Shadloo, Z. Yang, "Entropy Generation in a Circular Tube Heat Exchanger Using Nanofluids: Effects of Different Modeling Approaches," *Heat Transfer Engineering*, vol. 38, pp. 853-866, 2016.

[21] H. Yarmand, G. Ahmadi, S. Gharehkhani, S. Kazi, M. Safaei, M. Alehashem, A. Mahat, "Entropy Generation during Turbulent Flow of Zirconia-water and Other Nanofluids in a Square Cross Section Tube with a Constant Heat Flux," *Entropy*, vol. 16, pp. 6116-6132, 2014.

[22] F. A. Soomro, K. Z. H. Rizwan-ul-Haq, Q. Zhang, "Numerical study of entropy generation in MHD water-based carbon nanotubes along an inclined permeable surface," *Eur. Phys. J. Plus*, vol. 132, 2017

[23} B. Darbari, S. Rashidi, J. A. Esfahani, "Sensitivity analysis of entropy generation in nanofluid flow inside a channel by response surface methodology," *Entropy*, vol. 18, no. 52, 2016.

[24] M. M. Bhatti, T. Abbas, M. Mehdi, M. Rashidi, S. Mohamed, E. Ali, "Numerical simulation of Entropy Generation with thermal radiation on MHD Carreau Nanofluid towards a Shrinking Sheet," *Entropy*, vol. 18, no. 200, 2016.

[25] Y. A. J. Mohammad, R. S. Mohammad, A. Abdullah, K. N. Truong, P. B. F. Enio, "Entropy Generation in Thermal Radiative Loading of Structures with Distinct Heaters," *Entropy*, vol. 19, no. 506, 2017.

[26] M. R. Mohammad, N. Mohammad, S. S. Mustafa, Y. Zhighang, "Entropy Generation in a Circular Tube Heat Exchanger Using Nanofluids: Effects of Different Modeling Approaches," *J. Heat Transf. Eng.*, 2017.

[27] S. K. Das, S. U. Choi, T. Pradeep, "Nanofluids: science and technology," *Hoboken, NJ: Wiley*, p.397, 2007.

[28] K. F. V. Wong, O. D. Leon, "Applications of nanofluids: current and future," *Adv Mech Eng.* Vol. 2, pp. 1–11, 2010.

[29] S. Chol, "Enhancing thermal conductivity of fluids with nanoparticles" *ASME-Publications-Fed*, vol. 231, pp. 99-106, 1995.

[30] J. A. Eastman, et al., "Anomalously increased effective thermal conductivities of ethylene glycolbased nanofluids containing copper nanoparticles," *Applied physics letters,* vol. 78, pp. 718-720, 2001.

[31] M. A. Mansour, et al., "Numerical simulation of mixed convection flows in a square lid-driven cavity partially heated from below using nanofluid," *International Communications in Heat and Mass Transfer,* vol. 37, pp. 1504-1512, 2010.

[32] M. Sheikholeslami, "Influence of magnetic field on nanofluid free convection in an open porous cavity by means of Lattice Boltzmann method," *J. Mol. Liq.* Vol. 234. Pp. 364–374, 2017.

[33] M. Sheikholeslami, "Numerical simulation of magnetic nanofluid natural convection in porous media" *Phys. Lett. A.* vol. 381, pp. 494–503, 2017.

[34] D. Yadav, D. Lee, H. H. Cho, “The onset of double-diffusive nanofluid convection in a rotating porous medium layer with thermal conductivity and viscosity variation: a revised model,” *J. Porous Media*, vol. 19, pp. 31–46, 2016.

[35] Z. H. Khan, W. A. Khan, M. Hamid, H. Liu, “Finite element analysis of hybrid nanofluid flow and heat transfer in a split lid-driven square cavity with Y-shaped obstacle,” *Physics of Fluids,* vol. 32, Issue 9.

[37] M. A. Shermet, T. Grosan, I. Pop, “Free convection in a square cavity filled with a porous medium saturated by nano uid using Tiwari and Das nano uid model”, *Trans. Porous Media*, vol. 106, pp. 595-610, 2015.

[37] F. Mabood, S. Shateyi, M. M. Rashidi, E. Momoniat, N. Freidoonimehr, “MHD stagnation point ow heat and mass transfer of nano uids in porous medium with radiation, viscous dissipation and chemical reaction,” *Adv. Powder Technol.*, vol. 27, pp. 742-749.

[38] M. Ghalambaz, F. Moattar, M. A. Shermet, I. Pop, “Triple-diffusive natural convection in a square porous cavity,” *Trans. Porous Media,* vol. 111, pp. 59-79, 2016.

[39] A. Mahmoud, I. Mejri, M. A. Abbasi, A. Omri, “Analysis of MHD natural convection in a nano liquid-filled in open cavity with non-uniform boundary condition in the presence of uniform heat generation/absorption,” *Powder Technol.*, vol. 269, pp. 275-289.

[40] M. Ziaei-Rad, M. Saeedan, E. Afshari, “Simulation and prediction of MHD dissipative nano uid ow on a permeable stretching surface using articial neural network,” *Appl. Thermal Eng.*, vol. 99, pp. 373-382, 2016.

[41] M. Ziaei-Rad, A. Kasaeipoor, M. M. Rashidi, G. Lorenzini, “A similarity solution for mixedconvection boundary layer nano fluid ow permeable surface,” *J. Thermal Sci. Eng. Appl.*, vol. 9.

[42] D. Poulikakos, A. Bejan, B. Selimos, K. Blake, “High rayleigh number convection in a fluid overlaying a porous bed,” *Int. J. Heat Fluid Flow,* vol. 7, pp. 109–116, 1986.

[43] C. Beckermann, R. Viskanta, S. Ramadhyani, "Natural convection in vertical enclosures containing simultaneously fluid and porous layers," *J. Fluid Mech.* Vol. 186, pp. 257–284, 1988.

[44] C. L. Chen, C. H. Cheng, "Buoyancy-induced flow and convective heat transfer in an inclined arc-shape enclosure," *Int. J. Heat Fluid Flow*, vol. 23, pp. 823-830, 2002.

[45] M. November, M. Nansteel, "Natural convection in rectangular enclosures heated from below and cooled along one sideInt," *J. Heat Mass Transf.,* vol. 30, pp. 2433-2440, 1987.

[46] M. M. Ganzarolli, L. F. Milanez, "Natural convection in rectangular enclosures heated from below and symmetrically cooled from the sides," *Int. J. Heat Mass Transf.*, vol. 38, pp. 1063-1073, 1995.

[47] F. Moukalled, S. Acharya, "Natural convection in a trapezoidal enclosure with offset baffles," *J. Thermophys. Heat Transf.*, vol. 15, pp. 212-218, 2001.

[48] R. Chinnakotla, D. Angirasa, R. Mahajan, "Parametric study of buoyancy-induced flow and heat transfer from L-shaped corners with asymmetrically heated surfaces", *Int. J. Heat Mass Transf.*, vol. 39, pp. 851-865, 1996.

[49] A. C. Baytas, "Entropy generation for natural convection in an inclined porous cavity," *Int. J. Heat Mass Transfer*, vol. 43, pp. 2089–2099, 2000.

[50] K. L. Walker, G. M. Homsy, "Convection in a porous cavity," *J. Fluid Mech.* Vol. 87, pp. 449–474.

[51] A. Bejan, "On the boundary layer regime in a vertical enclosure filled with a porous medium," *Lett. Heat Mass Transfer*, pp. 693–102, 2011.

[52] Y. Varol, H. F. Oztop, T. Yilmaz, "Two-dimensional natural convection in a porous triangular enclosure with a square body," *Int. Commun.Heat Mass Transfer*, vol. 34, pp. 238-247, 2007.

[53] H. F. Oztop, I. Dagtekin, M. Duranay, "Analysis of natural convection problem in a cavity with partially heated and block inserted," *Proceedings of 13rd Heat Science and Technology Congress, Turkey*, pp. 217-222, 2001.

Figures

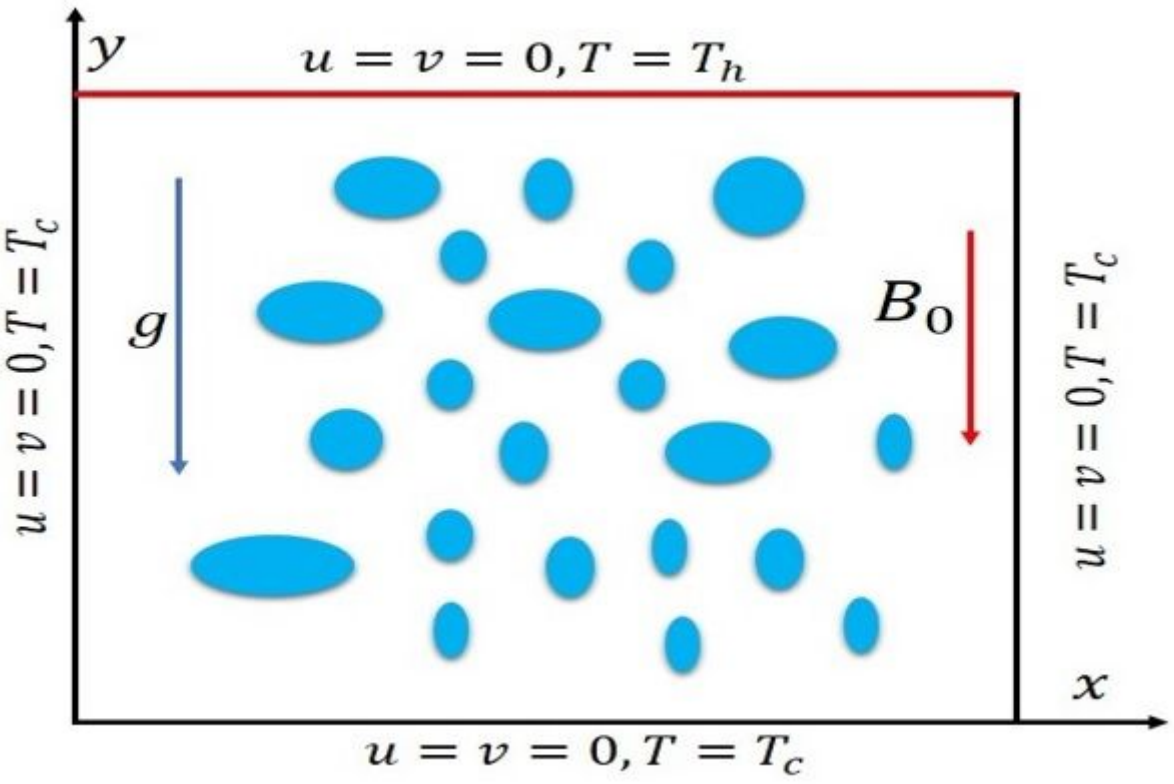

Figure 1

Physical structuring of problem.

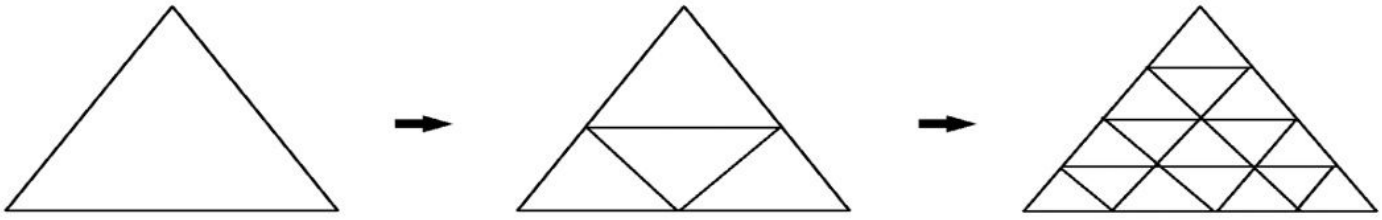

Figure 2

Sequence of grids on space mesh level: 1, 2, 3 (from left to right)

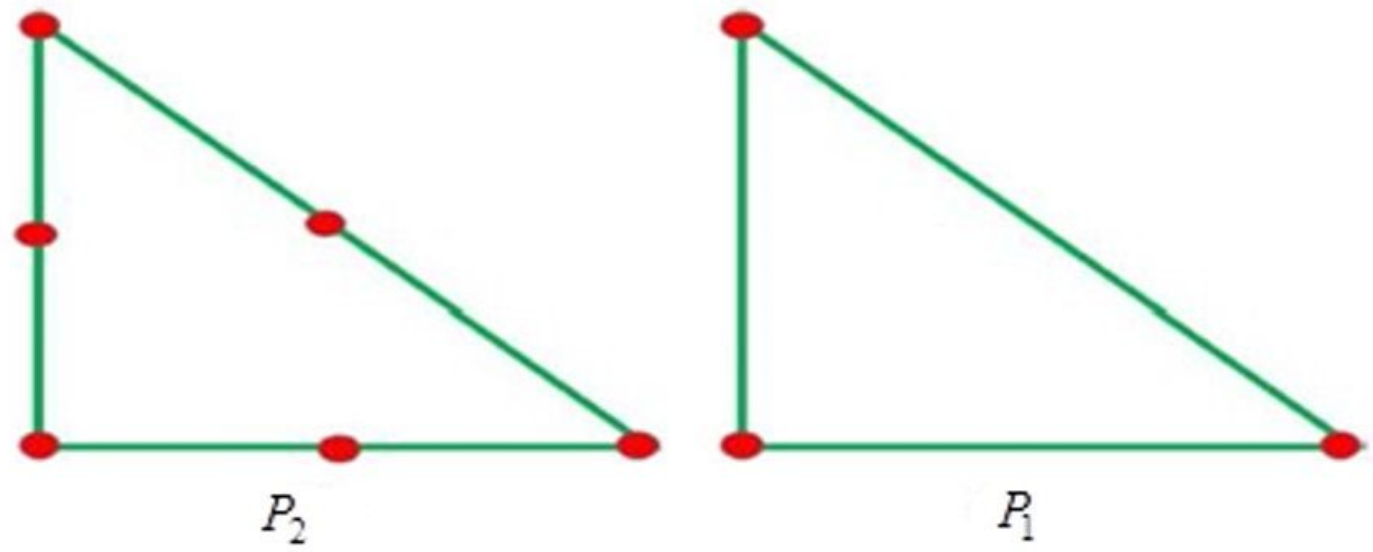

Figure 3

P2 - P1 finite element pair with placement of degrees of freedom.

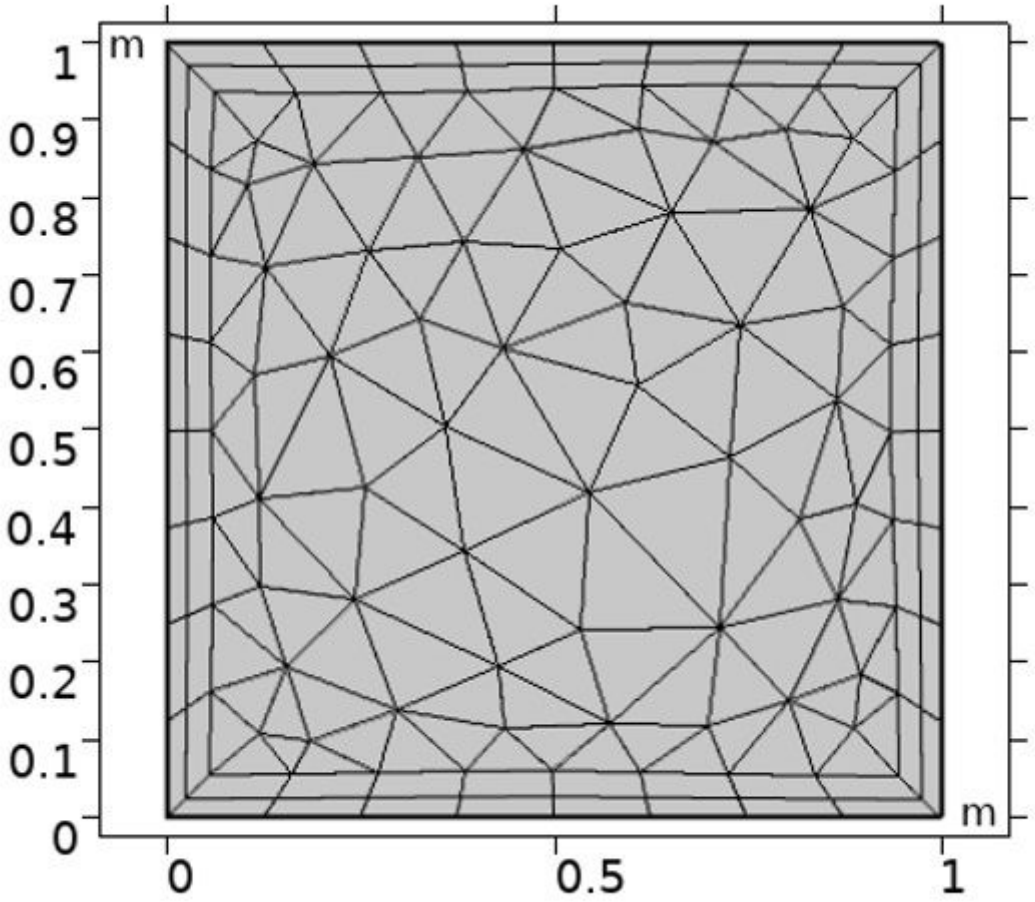

Figure 4

Discretization of computational domain

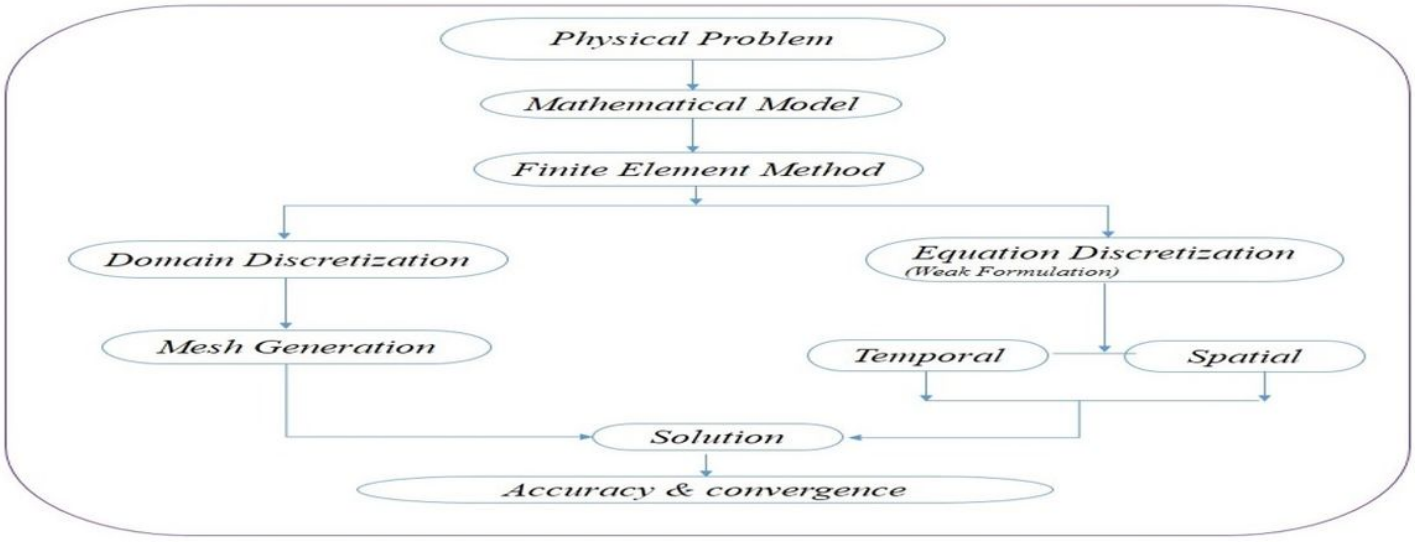

Figure 5

Step involved in implemented method.

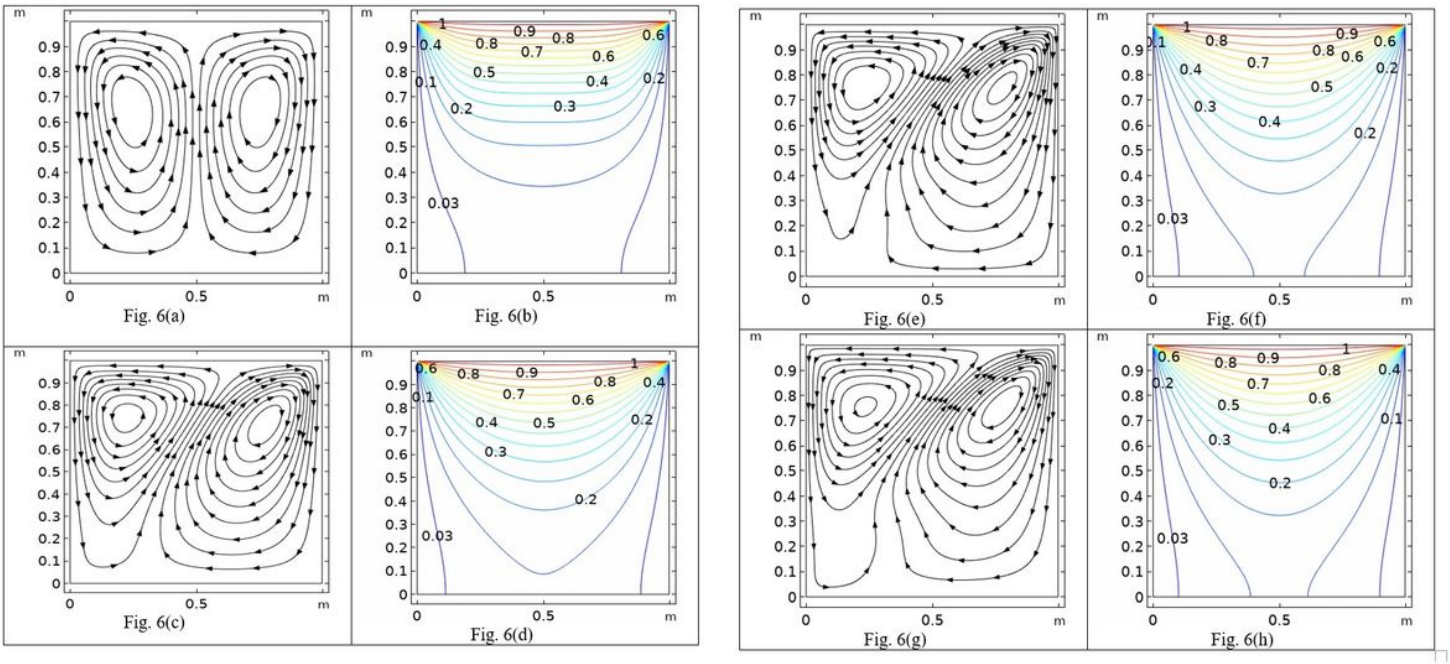

Figure 6

(a-h) Influence of Hartmann number (Ha) on streamline (Left) and isotherm (Right)

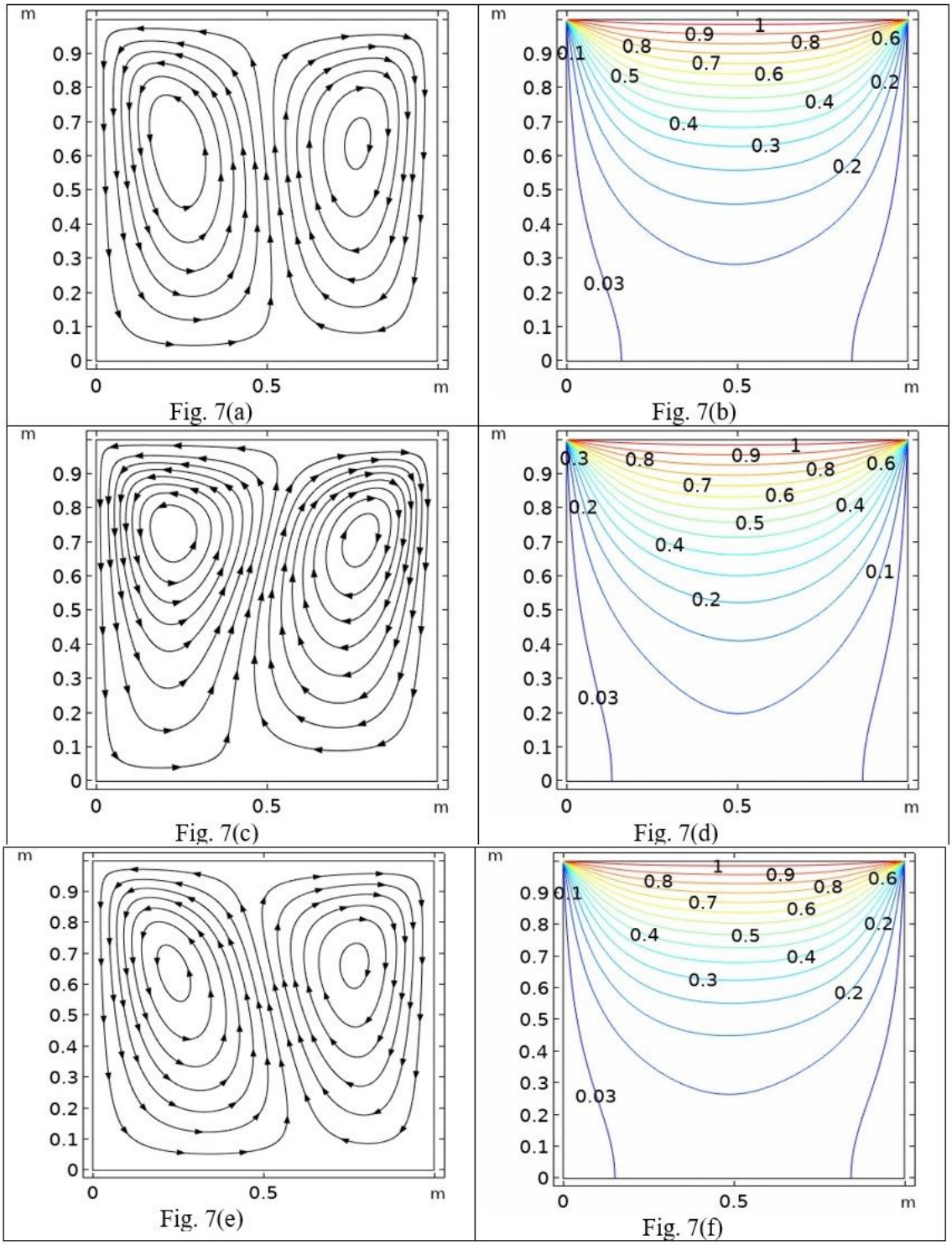

Figure 7

(a-f) Influence of magnetic field (γ) inclination for streamline (Left) and isotherm (Right).

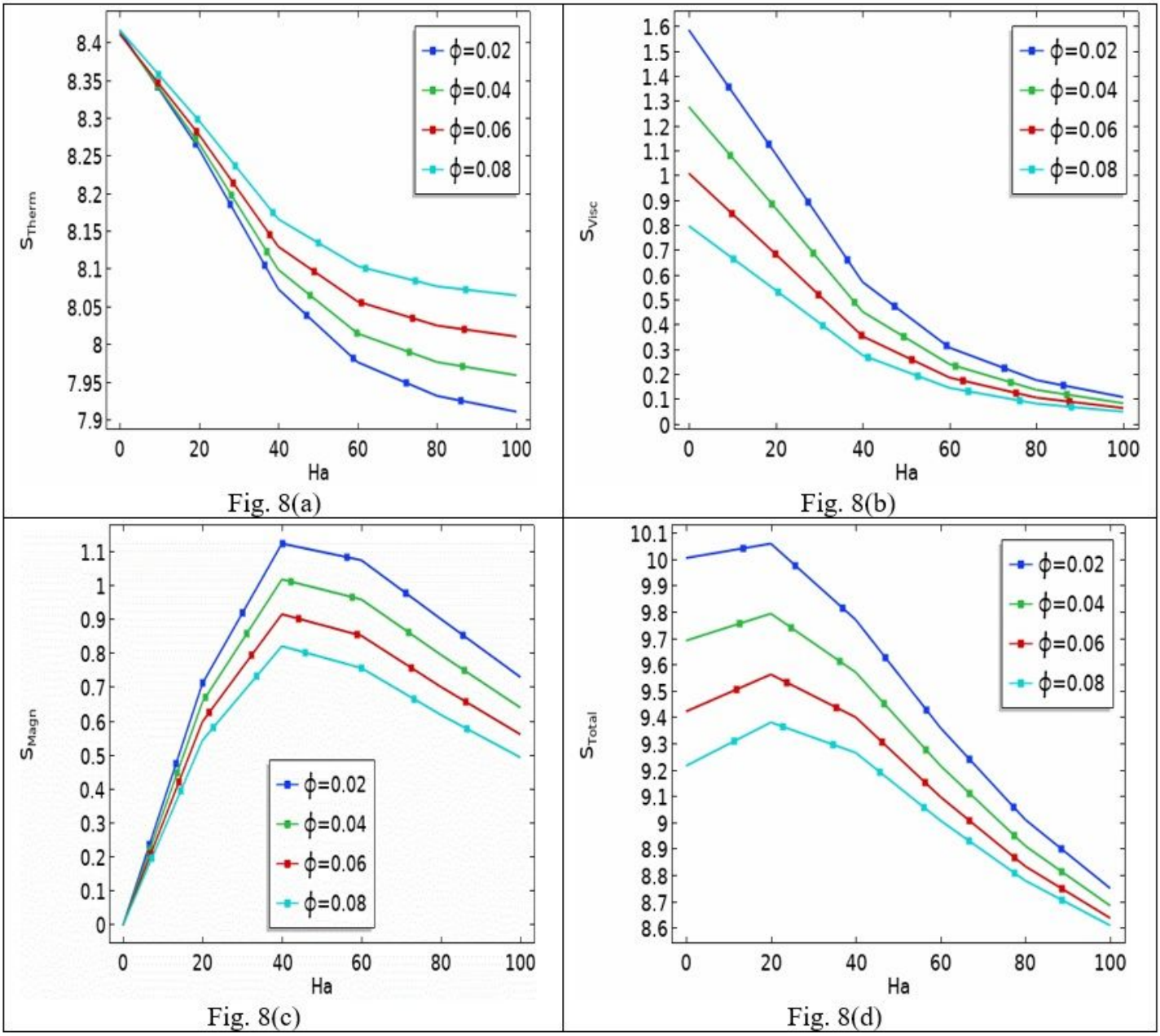

Figure 8

(a-d) Variation in entropy generation versus .

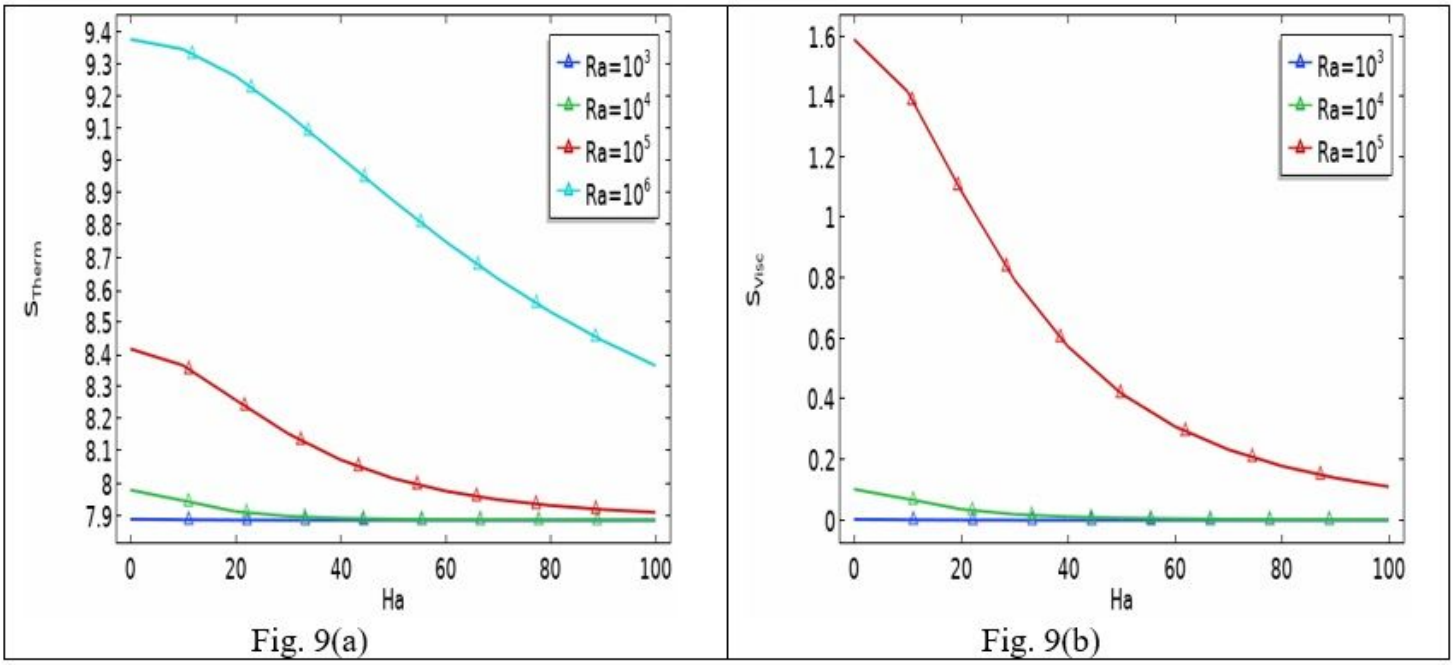

Figure 9

(a-b) Variation in entropy generation versus (Ra).

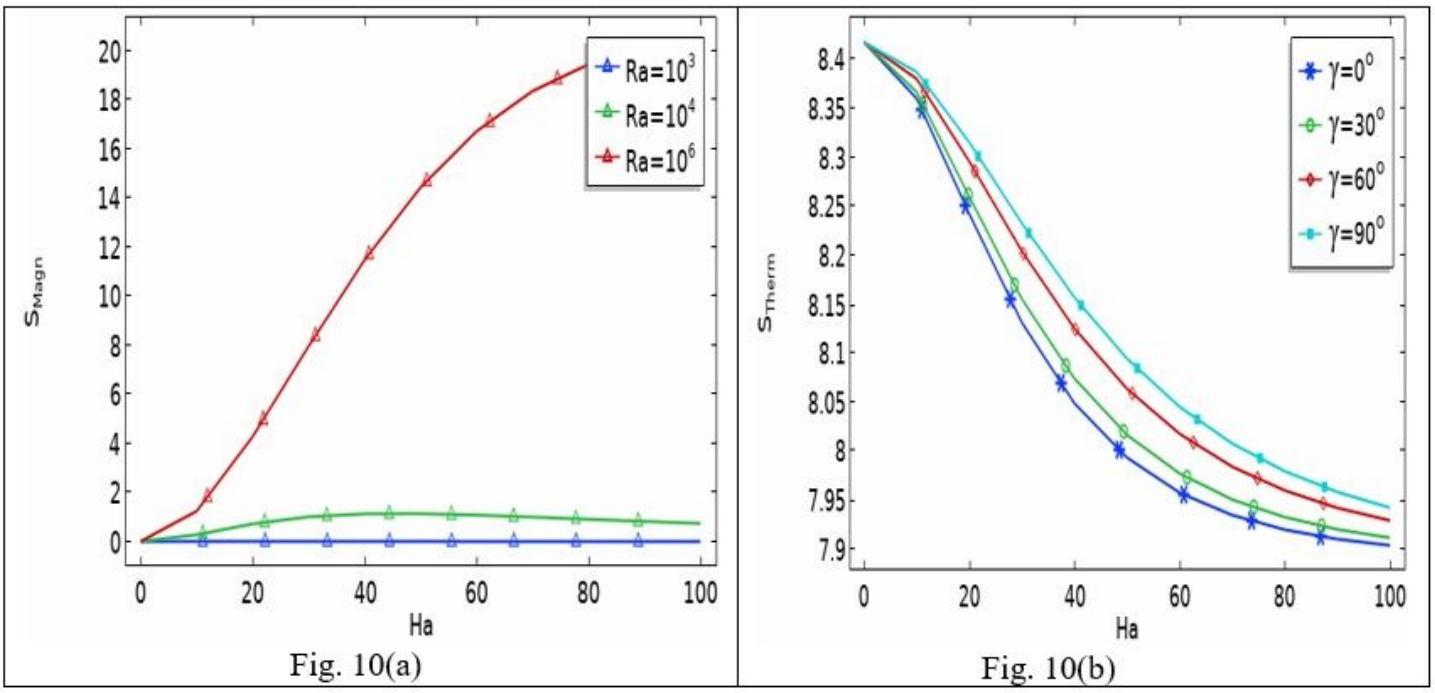

Fig. 10(a) Fig. 10(b)

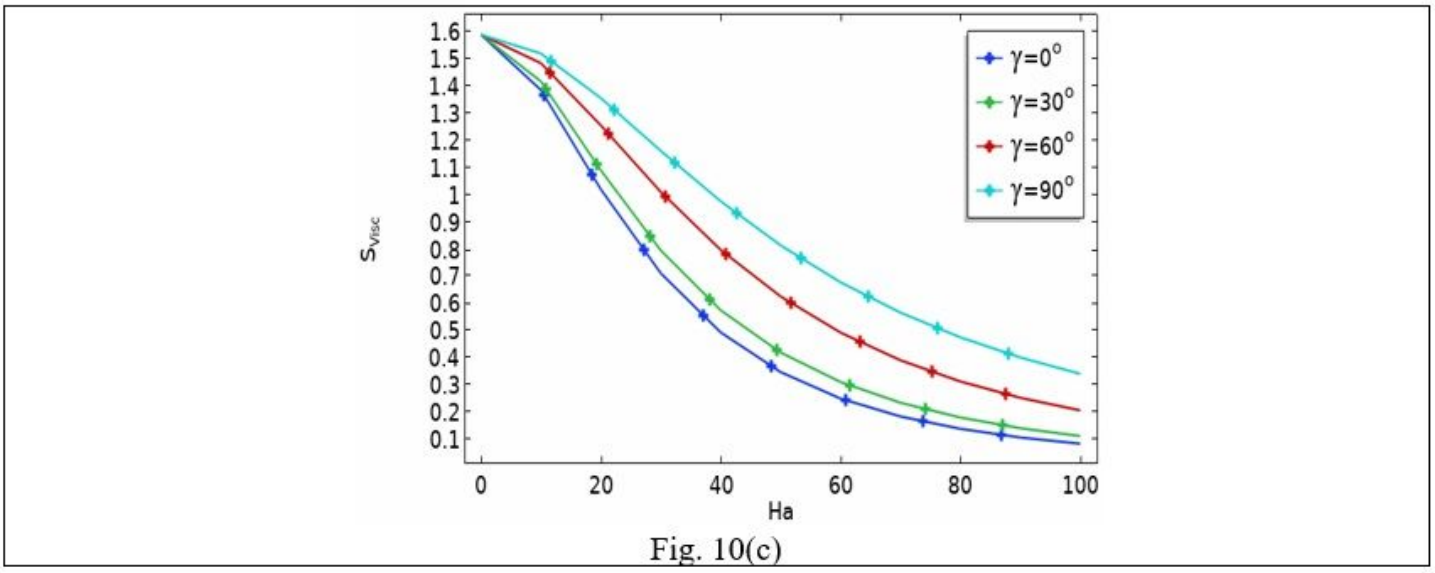

Fig. 10(c)

Figure 10

(a-c) Entropy variation against (□)

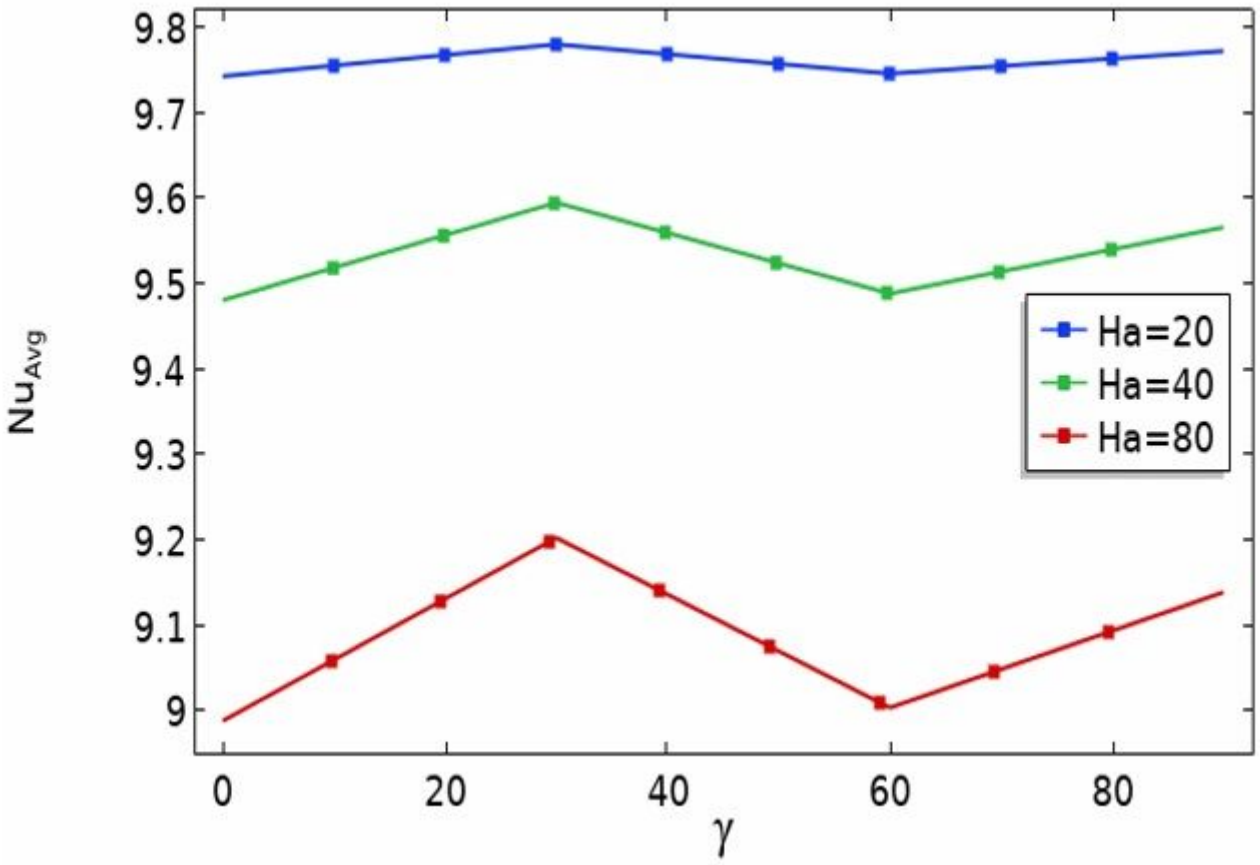

Figure 11

Influence on average Nusselt number for various Ha.